Lehrstuhl II für Mathematik

RWTH AACHEN UNIVERSITY

Diese Arbeit wurde vorgelegt am
Lehrstuhl II für Mathematik

Optimale Verkabelung von Heliostaten in Solarturmkraftwerken mittels ganzzahliger linearer Optimierung

Optimal Cable Routing of Heliostats in Solar Tower Power Plants Using Integer Linear Programming

Bachelorarbeit
Computational Engineering Science

März 2018

Vorgelegt von Presented by	Tanja von Platen Seilgraben 34-36 52062 Aachen Matrikelnummer: 334139 tanja.von.platen@rwth-aachen.de
Erstprüfer First examiner	Jun.-Prof. Dr. Christina Büsing Lehrstuhl II für Mathematik RWTH Aachen University
Zweitprüfer Second examiner	Prof. Dr. Arie Koster Lehrstuhl II für Mathematik RWTH Aachen University
Koreferent Co-supervisor	Dr. rer. nat. Pascal Richter Lehr- und Forschungsgebiet: Kontinuierliche Optimierung (IGPM) RWTH Aachen University

Eigenständigkeitserklärung

Hiermit versichere ich, dass ich diese Bachelorarbeit selbständig verfasst und keine anderen als die angegebenen Quellen und Hilfsmittel benutzt habe. Die Stellen meiner Arbeit, die dem Wortlaut oder dem Sinn nach anderen Werken entnommen sind, habe ich in jedem Fall unter Angabe der Quelle als Entlehnung kenntlich gemacht. Dasselbe gilt sinngemäß für Tabellen und Abbildungen. Diese Arbeit hat in dieser oder einer ähnlichen Form noch nicht im Rahmen einer anderen Prüfung vorgelegen.

Aachen, im März 2018

Tanja von Platen

Abstract

This thesis is concerned with the optimal cable routing of heliostats in solar tower power plants. Each heliostat in the field is connected to the solar tower via a data and a power cable, thereby providing the heliostat with information and power. The data and power cable optimization are seen as individual optimization problems and are solved independently.

The data cable model is initially formulated as a traveling salesman problem. Adding capacity constraints to the model, a further formulation as a capacitated vehicle routing problem is implemented. Two variations of the subtour elimination constraints are implemented and analyzed.

Furthermore, for the power cable model, different cable types are considered. At first, the problem is formulated as a capacitated vehicle routing problem using Miller-Tucker-Zemlin constraint formulations. The final model is defined as a distance and capacity constrained vehicle routing problem, taking all constraints of the power cable into account.

The data cable model is applied to an existent solar tower power plant, the PS10 in Seville, Spain. Computational results for the data cable optimization are compared to existing layouts obtained by heuristic methods. The power cable model is tested for a small test case.

Contents

Abstract iii

List of Figures vi

List of Tables vii

1. Introduction 1

2. Solar Tower Power Plants 3
2.1. Fundamentals . . . 3
2.2. Cost Model . . . 4
2.2.1. Data Cable . . . 4
2.2.2. Local Control Units . . . 4
2.2.3. Power Cable . . . 5
2.2.4. Labor Costs . . . 6

3. Modeling Fundamentals 7
3.1. Routing Problems . . . 7
3.2. Integer Linear Programming . . . 8
3.2.1. Optimality . . . 9
3.3. Solving the Optimization Problem . . . 9
3.3.1. Branch-and-Bound . . . 9
3.3.2. Acceleration Methods . . . 12

4. Data Cable Model 13
4.1. Modeling Approach . . . 13
4.2. Problem Formulation as TSP . . . 14
4.2.1. Computational Results . . . 17
4.3. Problem Formulation as CVRP . . . 20
4.3.1. Planarity Constraint . . . 21
4.3.2. Advantages of Parallelism . . . 24
4.3.3. Alternative Subtour Elimination Constraint Formulation . . . 24
4.3.4. Optimization using a Start Value . . . 25
4.4. Runtime Limitations . . . 27
4.4.1. CVRP Formulation for PS10 . . . 28
4.5. Result Evaluation and Conclusion . . . 29

5. Power Cable Model 32
5.1. Modeling Approach . . . 32
5.1.1. Miller-Tucker-Zemlin Formulation . . . 33
5.2. Problem Formulation as a DCVRP . . . 33
5.2.1. Capacity Restrictions . . . 35
5.2.2. Computational Results with Capacity Constraints . . . 36

5.2.3. Length Restrictions 39
5.3. Conclusion 40

6. Concluding Remarks **42**
6.1. Conclusion 42
6.2. Outlook 42

Appendix **44**

A. Power Cable Calculations **44**

B. Power Cable Length Approximation **45**

C. Recapitulation of All Power Cable Constraints **46**

List of Figures

2.1. Solar tower power layout . . . 3
2.2. Visualization of local control units. . . . 5
3.1. Example of a TSP . . . 7
3.2. Example of a VRP . . . 8
3.3. Branch-and-bound search tree. . . . 10
3.4. Branch-and-bound flow chart. . . . 11
4.1. Naive cable routing layout for PS10. . . . 17
4.2. Hamiltonian path cable routing layout for PS10. . . . 17
4.3. Optimal cable routing layout using exact methods. . . . 18
4.4. Cabling costs for each country. . . . 19
4.5. Example of crossing edges within a tour. . . . 21
4.6. Example of crossing edges for multiple routes. . . . 22
4.7. Flow chart for data cable optimization process. . . . 23
4.8. Parallel speedup over cores. . . . 24
4.9. Runtimes for subtour formulations OCC and ICC. . . . 25
4.10. Runtimes including start value. . . . 26
4.11. Relative gap including and excluding start value. . . . 27
4.12. Maximal heliostat optimzation within 6 h . . . 28
4.13. Incomplete CVRP model for PS10 . . . 29
4.14. Cable routing comparison for 5 tours. . . . 30
4.15. Cable routing comparsion for 2 tours . . . 30
5.1. Visualization of capacity constraint for the power cable. . . . 37
5.2. Optimized cable layout with two available cable types. . . . 38
5.3. Optimized cable layout with three available cable types. . . . 38
5.4. Example of the length restrictiont. . . . 40

List of Tables

2.1. Material costs for data cable. 4
2.2. Prices for local control units. 5
2.3. Costs for different power cable types. 6
2.4. Labor costs per country. 6
4.1. Overview of data cable constraints for the TSP formulation. 13
4.2. Overview of data cable constraints for the CVRP formulation. 14
4.3. Summary of data cable constraints, TSP formulation. 16
4.4. Cable routing comparisons for the data cable. 19
4.5. Summary of data cable constraints, CVRP formulation. 21
5.1. Overview of power cable constraints. 32
5.2. Example cable type capacities. 37
5.3. Summary of power cable constraints. 41
A.1. Overview of parameters used in power cable model. 44
B.1. Maximal cable length and capacity restriction for each cable type. . . . 45

1. Introduction

The importance of renewable energy is indisputable and the advancements being made in this sector are of great importance to reduce the dependency on fossil fuels. Solar power, as an inexhaustible energy source, is key to this process. A challenge however lies in extracting this energy cost-effectively and efficiently.

Of the different concentrated solar power (CSP) plants, the solar tower power plant yields promising commercial usage due to its high operating temperature and relatively small losses [**?**]. A big advantage is the energy storage ability, which allows energy demands to be met during peak periods - irrespective of the presence of sunlight. An additional advantage of solar tower power plants is the relatively low maintenance cost compared to fossil fuel generation plants. However, the large initial investment costs remain a deciding disadvantage, making up about 80 % of the entire cost. A lot of research has been invested in the optimization of the heliostat field, which accounts for up to 50 % of the installation cost of the entire power plant [**?**]. Reducing installation costs of solar tower power plants is therefore an important aspect in today's research on solar energy.

Researchers have made advancements in the optimization of the layout of the heliostat field, however, the actual cabling of the heliostats is still open to improvement. Efficiently laying the cables that supply the reflective mirrors with power and data, can lead to noteworthy cost savings.

The possible cost savings are demonstrated in an initial approach using heuristic methods. The approach is discussed in a previous bachelor thesis, showing that roughly 18 % in total costs for the data cable and 20 % for the power cable could be saved [**?**]. Results are obtained in a short amount of time, therefore providing heuristic methods with an advantage when runtime is a limiting factor. Furthermore, an exact approach to cable routing was implemented whilst searching for the optimal connections of offshore wind farms. The problem was formulated as an integer linear program (ILP) and solved using optimization solvers. A successful implementation for different test cases was possible and resulted in savings of between 14 % and 25 % [**?**].

The optimization problem discussed in this thesis refers to the cable connections between the heliostats and can be described as a routing problem. The traveling salesman problem (TSP) and the vehicle routing problem (VRP) are two well-known routing problems that have been extensively researched. Applying the concept of the traveling salesman problem to a variety of fields, has greatly contributed to solving combinatorial optimization problems [**?**].

Formulating the problem of this thesis as an ILP and using the optimization solver Gurobi, the goal is to find the optimal cable routing of a solar tower power plant under consideration of connection and cabling costs. This approach will be applied to the

PS10, an existing solar tower power plant in Seville, Spain, consisting of 624 heliostats. The breakdown of the problem results in independent models for the data and power cable. The intention is to model the problem as realistically as possible. Later a comparison of the exact and heuristics approach will be made.

The thesis is divided into five sections, starting with an introduction to the fundamentals of solar tower power plants and the incurring cabling costs in Section 2. Thereafter, in Section 3, the mathematical fundamentals of integer linear programming are discussed. Additionally, the optimization solver and the exact methods used by the solver are described. Section 4 and Section 5 detail the data cable and power cable model respectively. Finally, the conclusion and outlook are given in Section 6.

Simulations were performed with computing resources granted by RWTH Aachen University under project thes0383.

2. Solar Tower Power Plants

A brief introduction to the setup and fundamentals of solar tower power plants will be given. Along with the fundamentals, the required cables, that are optimized in the routing problem, will be described in further detail.

2.1. Fundamentals

A solar tower power (STP) plant consists of two main elements - the central receiver tower and reflecting mirrors surrounding the tower, as shown in Fig. 2.1. The mirrors, known as heliostats, bundle the sunlight and focus it onto the receiver located at the top of the tower. The central receiver absorbs the highly concentrated solar irradiation and converts it into heat. The heat is transferred to a heat transfer medium, either molten salt or hot air, which powers a steam turbine to generate electrical energy [**?**]. The layout of the field is optimized with the intention of gaining maximal thermal energy [**?**].

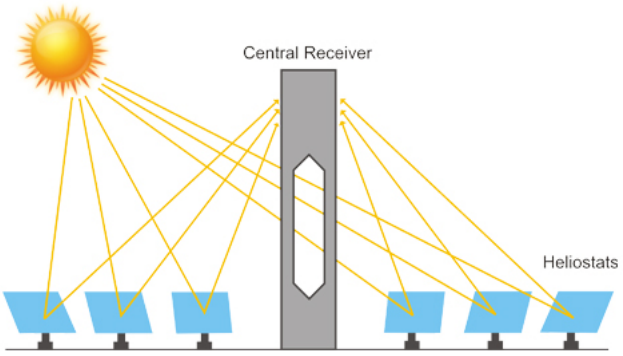

Figure 2.1: Solar tower power plant layout, taken from [**?**]. Solar radiation is reflected by the heliostats to a central receiver located at the top of the solar tower.

The heliostats are connected to the central receiver tower by means of two cables - the data and power cable. The data cable is responsible for sending information to the heliostats, e.g. data on the current position of the sun. Furthermore, the heliostats are equipped with a dual-axis tracking motor to achieve optimal positioning when tracking the sun. The 100 W motor installed at the mirrors is powered by the power cable.

The PS10, the solar tower power plant model being used in this thesis, encompassed a surface area of 50 ha of which the reflective surface covers 75 000 m^2 [**?**]. In terms of communication and powering of the heliostats, an attempt at a wireless implementation has been researched. The complexity, however, remains high and with a moderate increase in size, the transmission ranges and data rates that are necessary, can be problematic [**?**].

Consequently, the method currently being implemented and the topic of this thesis, will use data and power cables to transfer the necessary information and power. The cost model for both cables is presented in the following section.

2.2. Cost Model

The costs can be divided into cabling, switch and labor costs. An overview is given in the following section. The cost predictions were made in collaboration with the company TSK Flagsol [**?**]. Note that all prices are provided in Euro and reduction in costs when ordering in bulk is not considered.

2.2.1. Data Cable

For the data cable two different cable types are available, namely the copper ethernet cable and the fiber optic cable, which will hence be referred to as copper and fiberglass cable, respectively. Cables are covered by protective foil to shield from environmental impacts and interference [**?**].

		Prices [€/m]
Cable	Fiberglass cable	2
	Copper cable	0.7
Additional material	Protective foil	2

Table 2.1: Material costs for the data cable. Prices given per meter.

As can be seen, the cost of fiberglass cable is notably higher than that of copper. However, the deciding disadvantage of copper is the length restriction of 100 m. Moreover, copper allows a connection of only two consecutive heliostats. Fiberglass cable is generally not restricted in length, nonetheless, protocols exist limiting the number of connected heliostats per subnetwork [**?**]. An overview of all data cable constraints can be found in Section 4.1.

2.2.2. Local Control Units

Further costs incur with the installation of different switches, also referred to as local control units (LOCs). A LOC is fitted at each heliostat and allows the data transfer to and between the heliostats. When installing the switches, it is important to bear in mind the high temperature regions that solar tower power plants are typically built in. Consequently, switches with working temperatures of up to 80°C should be fitted [**?**]. The available switches and their prices per unit are listed below in Table 2.2.

LOC	Price/piece [€]
Endpoint	10
Conductor	100
8-port fiberglass	800
8-port copper	800
16-port fiberglass	1500
16-port copper	1500

Table 2.2: Prices for local control units.

The different types of LOCs are depicted in Fig. 2.2, whereby fiberglass is represented in blue and copper in red. A multi-port switch has one incoming cable and branches out into n outgoing cables, each outgoing cable connecting a further heliostat.

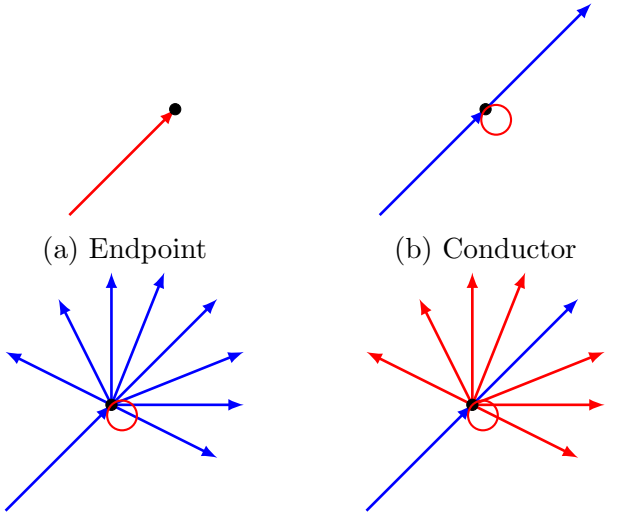

(a) Endpoint (b) Conductor

(c) Multi-port fiberglass (d) Multi-port copper

Figure 2.2: Different types of local control units used for data transmission. Copper cable is represented in red and fiberglass in blue. A heliostat is represented by a black point.

Note that each heliostat is connected to a copper cable, that supplies the heliostats with information. This does not affect the cable routing and costs are included in the price of the LOC.

2.2.3. Power Cable

As multiple heliostats are supplied by one cable, a capacity restriction for the power cable should be applied. Additional costs, in terms of switches, do not need to be taken into account. However, the costs for protective foil, as mentioned in Table 2.1, should be considered. Cables with different current ratings are used in the layout, with the

prices per meter listed in the following table.

t	**Cable type**	**Current rating r^t [A]**	**Cable capacity h^t**	**Prices [€/m]**
1	NYY-J 3 x 2.5 RE	36	56	0.58
2	NYY-J 3 x 4 RE	47	73	0.87
3	NYY-J 3 x 6 RE	59	92	1.24
4	NYY-J 3 x 10 RE	79	124	1.95
5	NYY-J 3 x 16 RE	103	162	3.13
6	NYY-J 3 x 25 RM	133	209	5.19
7	NYY-J 3 x 35 RM	159	250	6.90

Table 2.3: Current ratings, cable capacities and costs per meter of the seven different cable types, [**?**].

Calculations concerning the maximal heliostats number (cable capacity h^t) can be found in Appendix (A), along with the relevant parameter values.

2.2.4. Labor Costs

The last element in the cost model, presenting the dominating cost factor, is the labor cost. As further CSP plants are planned in Australia and the UAE, the labor costs for these countries are listed as well. A great variation in labor costs is mainly due to the minimum wage of each country. The dimensions of the cable trenches are assumed to be one meter in depth and one meter in width. The costs are estimated for medium-hard soil.

Country	**Costs [€/m]**
Spain	25
South Africa	10
Australia	50
United Arab Emirates	10

Table 2.4: Labor costs per country [**?**].

3. Modeling Fundamentals

The aim of an optimization problem is to find the best solution to a given problem, e.g. minimum cost implications or maximal route length [**?**]. In this thesis, the aim is to optimize the cable routing, while minimizing the overall costs. This section begins with a brief review of routing problems and thereafter gives the mathematical formulation of optimization problems.

3.1. Routing Problems

Routing problems can be described with the help of graph theory terminology. Consider a graph $G = (V, E)$, whereby V is a set containing all n vertices, or nodes, and E a set containing all edges. An edge is defined by two connecting vertices $(i, j) \in V$ and is referred to as an arc if the edge has a direction. A graph consisting of directed edges is said to be a digraph. Additionally, a graph containing no crossings is referred to as a planar graph [**?**].

The traveling salesman problem (TSP), see Fig. 3.1, is described by a tour through n cities, by which the cities are represented by vertices and the route traveled is represented by edges. In case of the asymmetric TSP, $(i, j) \neq (j, i)\ \forall\ i, j \in V$, the traveled route is illustrated by arcs. A tour is defined as a sequence of vertices with no repeated edges. The intention of the TSP is to find the shortest tour through all n cities, starting and ending at the same node [**?**].

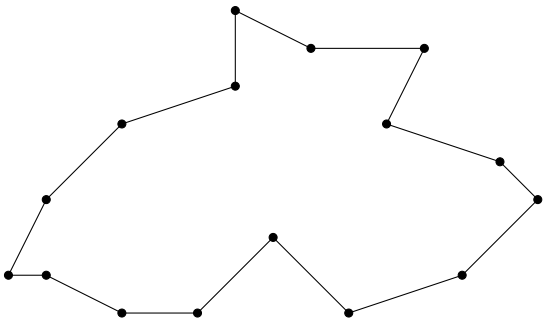

Figure 3.1: Example of a traveling salesman problem with $n = 16$.

A further routing problem, the so-called vehicle routing problem (VRP), is illustrated in Fig. 3.2 and is a generalization of the TSP. The VRP is defined to consist of n customers and m vehicles located at a depot. Similar to the TSP, the VRP aims to determine the shortest tour, with the addition of m tours starting from the depot [**?**]. A generalization of the VRP is the capacitated VRP, which restricts the number of customers each vehicle is allowed to visit during its tour.

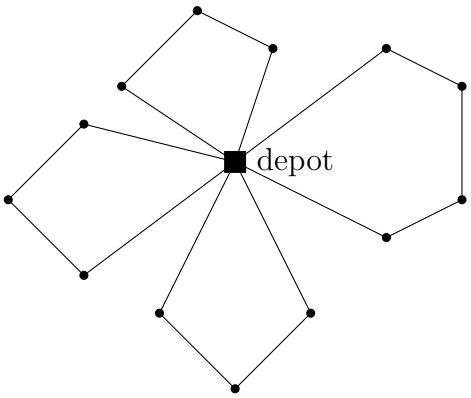

Figure 3.2: Example of a vehicle routing problem with $n = 13$ and $m = 4$.

The VRP belongs to the complexity class of $\mathcal{NP}$-hard problems, while the TSP belongs to the class of $\mathcal{NP}$-complete problems. A class is said to be in $\mathcal{NP}$ if it can be verified by a polynomial-time algorithm. The TSP is $\mathcal{NP}$-complete as it is in $\mathcal{NP}$ and any instance of another problem, such as the VRP, can be reduced to the TSP in polynomial time. Since the VRP is not necessarily in $\mathcal{NP}$ but can be reduced to the TSP in polynomial time, it is $\mathcal{NP}$-hard [**?**]. As such, a VRP can be very difficult to solve.

Obtaining an optimal route for the VRP and TSP, they are first formulated with the help of integer linear programming (ILP), explained in the next section. Thereafter, the optimization problems can be solved with the branch-and-bound method, described in Section 3.3.

3.2. Integer Linear Programming

The goal of solving an optimization problem can be defined as minimizing or maximizing an objective function under a set of given constraints [**?**]. The formulation as a linear program can be divided into three parts, namely the variables to be optimized, the objective function and the constraints [**?**].

The variables, e.g. what resource to use or what path to take, make up the solution. The objective function, describing the function to be minimized or maximized, is dependent on the variables. Lastly, the variable choices are restricted by the defined constraints, which describe the structure of a problem.

Collectively, the formulation for a minimization problem is thus defined by,

$$\begin{aligned} \min \quad & c^T x \\ \text{s.t.} \quad & Ax \leq b \\ & x \geq 0 \end{aligned} \tag{3.1}$$

whereby $A \in \mathbb{R}^{m \times n}$, $c \in \mathbb{R}^n$, $b \in \mathbb{R}^m$ and $x \in \mathbb{Z}^{n-q} \times \mathbb{Q}^q$. If x is integer, $q = 0$ and the problem is defined as an integer linear program. For $n = q$, the problem is known as a linear program (LP) [**?**]. Furthermore, restricting the variables to only binary values, the problem is known as a binary optimization problem (BIP) [**?**].

3.2.1. Optimality

A solution $x^* \in X \subset \mathbb{Z}^{n-q} \times \mathbb{Q}^q$ can be said to be optimal when $\overline{z} - \underline{z} \leq \epsilon$, with $\overline{z}$ and $\underline{z}$ defining an upper and lower bound on the solution, respectively. The ϵ is a suitably chosen small non-negative value and X defines the feasible region [**?**].

For the purpose of finding the lower and upper bounds, consider the ILP to be given by,

$$z = \min \{c(x) \mid x \in X \subseteq \mathbb{R}^n\}. \tag{3.2}$$

The lower bound, $\underline{z} = c(x^*) \geq z$, is any feasible solution $x^* \in X$. The upper bound is found by way of relaxation. Consider the following, denoting a relaxation of Eq. (3.2), if $X \subseteq T$ and $f(x) \leq c(x)\ \forall x \in X$,

$$z^R = \min \{f(x) \mid x \in T \subseteq \mathbb{R}^n\}.$$

Consequently, if $z^R \leq z$ a relaxation of the ILP is given. This is true, since $x^* \in T$ and hence $f(x^*)$ is a lower bound on the relaxation z^R, leading to the statement $z \geq f(x^*) \geq z^R$ [**?**].

3.3. Solving the Optimization Problem

Having formulated the problem as an ILP, the optimization problem can subsequently be solved by the branch-and-bound method, described in the upcoming section. Further methods to accelerate the solution process are discussed thereafter.

3.3.1. Branch-and-Bound

The optimization solver Gurobi, makes use of the linear programming based branch-and-bound algorithm [**?**] and will thus be used to solve the cable routing problem. Gurobi is a mathematical programming solver that takes advantage of modern day computer architectures and is so able to efficiently utilize mutli-core processors. Moreover, the Gurobi optimization library can easily be used in conjunction with Matlab.

The idea behind the algorithm, is to divide the problem into smaller problems which will be easier to solve. This can be seen as a divide and conquer approach. Based on the description found in [**?**], regard the problem

$$z = \min \{cx \mid x \in S\}.$$

The set S can be divided into reduced sets $S = S_1 \cup S_2 \cup ...S_k$ and the sub-problems then defined by $z^k = \min \{cx \mid x \in S_k\}$ for $k = 1..K$. Subsequently, it holds that $z = \max_k z^k$. What follows is an enumeration tree, as shown in Fig. 3.3.

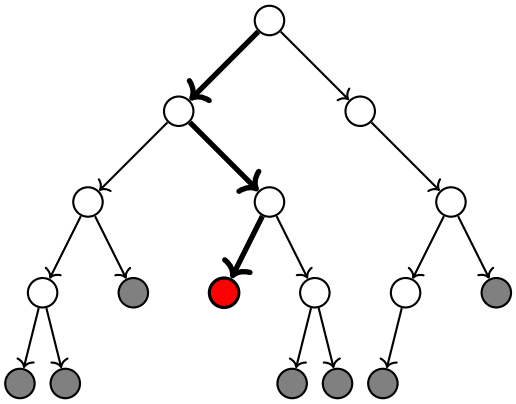

Figure 3.3: Branch-and-bound search tree. The gray nodes represent fathomed nodes and the red node the active node.

The branch-and-bound tree would quickly become excessively large if complete enumeration was undertaken, therefore, conditions are needed that limit the size of the tree. Bounds on the values of z^k are required. The upper bound is obtained via LP relaxation, attained by removing the integrality constraints of the ILP problem, as described in Section 3.2.1. The relaxation of the LP is solved by the dual simplex algorithm. When re-optimizing the LP at each node, the dual simplex method can be used without having to find a new lower bound [**?**]. For a more in-depth look at the algorithm, refer to [**?**],[**?**]. The lower bound is initially set to $\underline{z} = \infty$, as no feasible solution is known at this stage.

For each node a modified LP needs to be solved, adding new restrictions at each node. Thereafter, each node is inspected, referred to as the active node, to discern if fathoming is possible. This would implicate that the node will not be branched on further. Reasons for fathoming of nodes can be,

(i) An optimal solution has been found

(ii) The resulting LP becomes infeasible, $S_k = \emptyset$

(iii) Bounding conditions, $\overline{z}^k \leq \underline{z}^k$.

A LP can become infeasible if the added restrictions lead to an infeasible solution. If the solution of a LP is integer, the best current feasible solution, the lower bound, can be updated and there is no need to branch further. This would be fathoming by optimality. Additionally, the incumbent $x^* \in X$ can be updated, which is a void vector at the start of the process. The last condition, fathoming by bound, ensures that if

the obtained optimized LP value is worse than the lower bound, the node is fathomed. A detailed flow chart can be found in Fig. 3.4.

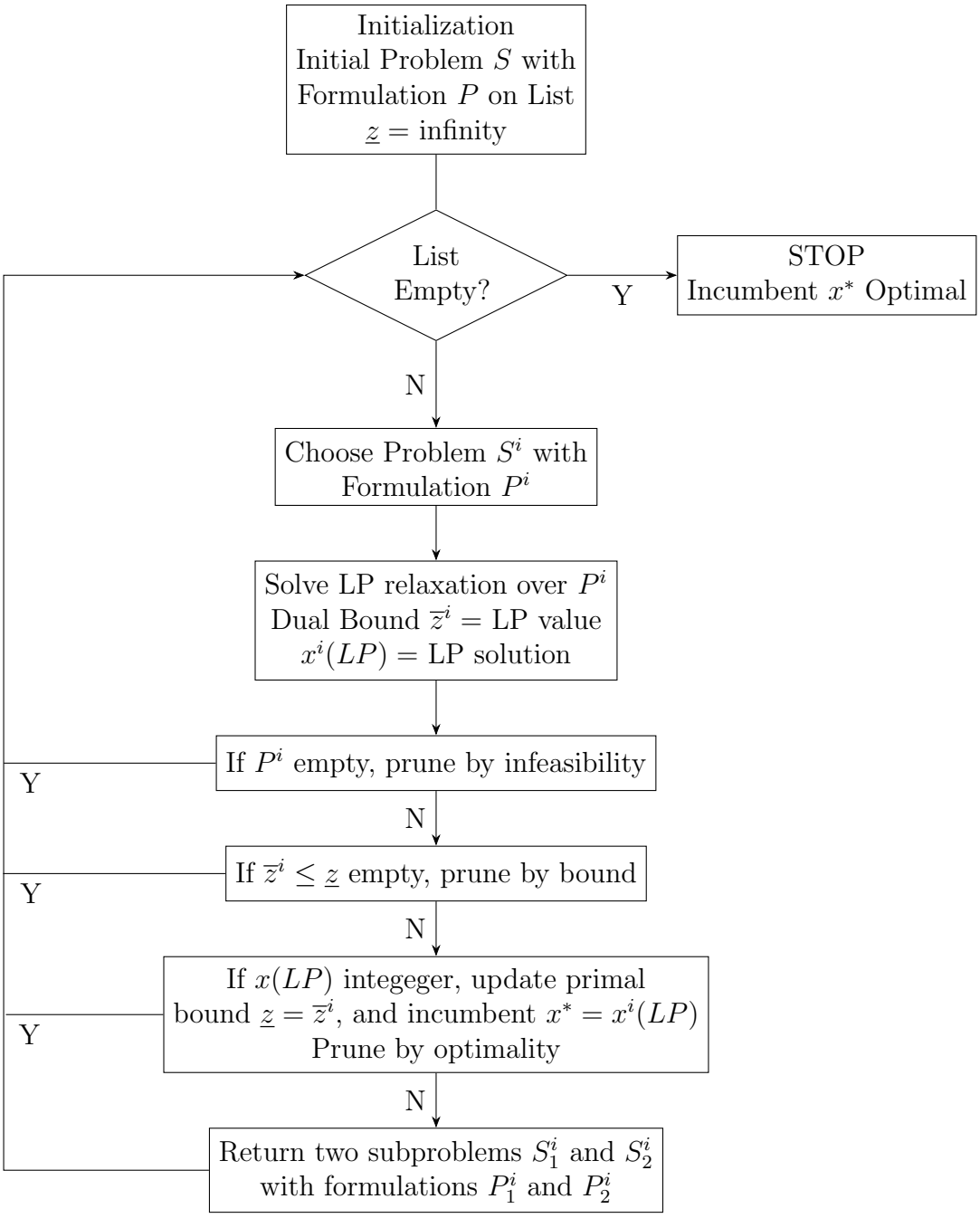

Figure 3.4: Branch-and-bound flow chart, detailing the process of finding an optimal solution. Adapted from [**?**].

3.3.2. Acceleration Methods

The goal of the acceleration methods are to limit the size of the search tree and therewith reduce the searching process and search time. The presolve method helps tighten the formulation and can be applied before the branch-and-bound method. It reduces the problem size and therefore also accelerates the search for the optimal solution.

The cutting planes method is responsible for many of the computational advancements that have been made in solving ILPs [**?**]. In essence, the idea is to remove undesirable fractional results during the solution process and do this without creating additional sub-problems (which merely make the search tree larger). The cuts are made during the solution process, as it is far too costly to find all possible constraints beforehand and also adding them to the matrix would make the LP relaxation harder to solve.

Moreover, Gurobi makes use of a range of heuristic methods. Adding a heuristic to the method could deliver a good incumbent value, which leads to branches being fathomed earlier on. Therefore, ultimately speeding up the search.

Lastly, the branch and bound tree has independent sub-problems, which can be solved in parallel. When dealing with large problems this is very useful, as much of the computation time is spent solving the sub-problems. However, if the problem is solved at or near the root node, parallelism is restricted and will not be able to speed up the process [**?**].

4. Data Cable Model

The optimization of the data cable is described in the following subsections. Section 4.1 gives an overview of the constraints, while Section 4.2 describes the cable routing as a TSP. Adding a further constraint in Section 4.3, the model is formulated as a capacitated VRP (CVRP).

4.1. Modeling Approach

Foremost, the constraints for the data cable are introduced. Topology constraints are not considered in this model and so the model can be seen as two-dimensional. Additionally, branching at the heliostats will not be allowed. The extensive cost of multi-port switches, which would have to be installed at each heliostat, incur a significantly higher cost. An approach using 8-port switches has been evaluated in the heuristics approach and resulted in an overall higher cost [**?**].

The objective of the optimization problem is to minimize the total costs. Under the following considerations, the model can be formulated as a TSP, see Section 4.2, or as a CVRP, see Section 4.3.

In Table 4.1 and 4.2, an overview of all constraints along with the cost model is given.

Formulation	**Constraint**	**Cost model**
TSP	• All heliostats are connected to the receiver tower • All heliostats are connected by one incoming and one outgoing cable • All heliostats are continuously connected	• Cable type fiberglass considered only • LOC of type conductor considered only • Consideration of installation costs, i.e. protective foil and labor costs

Table 4.1: Overview of data cable constraints and cost model for the TSP formulation.

Formulation	Constraint	Cost model
CVRP	• All heliostats are connected to the receiver tower • All heliostats are connected by one incoming and one outgoing cable • All heliostats are continuously connected • Cable crossings are forbidden • Maximum attendance number of heliostats per cable limited to $h_{max} = 128$	• Cable type fiberglass considered only • LOC of type conductor considered only • Consideration of installation costs, i.e. protective foil and labor costs

Table 4.2: Overview of data cable constraints and cost model for the CVRP formulation.

4.2. Problem Formulation as TSP

Consider a a fully connected graph $G = (V, A)$ with a set of vertices $V = \{1, ..., n\}$ representing the heliostats in the field and vertex $n = 1$ representing the solar tower. An additional set is defined by $\bar{V} = V \setminus \{1\}$. The set, $S \subset V$, is defined to contain the tours violating the subtour elimination constraint. The set A defines a set of arcs, by which every arc (i, j) with $i \neq j$ is associated with a non-negative cost matrix $c_{i,j}$. The cost matrix is defined by the distance matrix $d_{i,j}$ and the incurring labor and material costs. The distance matrix is defined by,

$$d_{i,j} = \sqrt{(x_i - x_j)^2 + (y_i - y_j)^2}.$$

The cost matrix can therefore be described by,

$$c_{i,j} = d_{i,j} \cdot \hat{c}$$

$$\text{with} \quad \hat{c} = c_{\text{labor}} + c_{\text{cable}} + c_{\text{protectiveFoil}}.$$

Further costs, with no relation to the distance however, are the conductor switch costs. A switch of type conductor is needed at each heliostat.

$$c_s = c_{\text{conductor}} \cdot n_{\text{heliostats}}$$

A modification to the standard TSP is made, as a returning edge is not required and will be removed in the final solution. The modified cost matrix is then defined by,

$$c_{i,j} = \begin{cases} c_{i,j} & \forall i \in V, j \in \bar{V} \text{ and } i \neq j \\ c_{i,1} & \forall i \in \bar{V}, i \neq j. \end{cases}$$

The returning edge should not affect the layout of the tour, hence all possible connection costs from the heliostats to the tower are set to the same large value $c_{i,1} = M$, $M \in \mathbb{R}$.

Besides the fiber optic cable, copper cable can be used for the cable routing of the data cable. However, the copper cable can connect only two succeeding heliostats and consequently could only be installed for the last two heliostats on the route (returning edge having been removed). For a TSP tour, this would result in a negligible cost advantage overall and is therefore not considered in this model.

Having defined the necessary cost matrix and sets, the model can be formulated as follows. Let m represent the number of outgoing cables from the solar tower and $x_{i,j}$, $(i \neq j)$ be a binary variable with,

$$x_{i,j} = \begin{cases} 1 & \text{if heliostat } i \text{ is connected to heliosat } j \\ 0 & \text{otherwise.} \end{cases}$$

The model then reads,

$$\min \sum_{\substack{i,j \in V \\ i \neq j}} c_{i,j} \cdot x_{i,j} + c_s \tag{4.1}$$

$$\text{s.t.} \sum_{\substack{i \in V \\ i \neq j}} x_{i,j} = 1 \qquad \forall j \in \bar{V} \tag{4.2}$$

$$\sum_{\substack{j \in V \\ i \neq j}} x_{i,j} = 1 \qquad \forall i \in V \tag{4.3}$$

$$\sum_{\substack{i \in S \\ j \in V \setminus S \\ i \neq j}} x_{i,j} \geq 1 \qquad \forall S \subset \bar{V}, S \neq \emptyset$$

$$x_{i,j} \in \{0,1\} \qquad \forall i,j \in V \qquad (4.4)$$

Constraint (4.2) and (4.3) are known as in and out degree constraints and ensure that each heliostat has exactly one incoming and one outgoing cable respectively. The constraint defined by (4.4) is known as the subtour elimination constraint (SEC). The SEC is added to the constraint matrix only after a first instance of the layout has been obtained. Adding constraints for all possible subtours would result in approximately 2^n inequalities for an n-heliostat field [**?**]. As shown in Algorithm 4.1, in order to deal with the exponential amount of SECs, an iterative approach is implemented.

Consider the obtained layout after all but the subtour elimination constraints have been added. After finding all subtours, add those which violate the subtour elimination constraint to the constraint matrix. Solve again and if the SEC is not violated,i.e, no tour is separate from the solar tower, an optimal solution has been found. In the negative case, the process of adding violated subtour constraints is repeated and solved again.

Input : Instance violating subtour constraints
Output: Optimal solution with m tours, each of capacity h_{max}
while *Subtour elimination constraints violated* **do**
  for *Subtour with violations* **do**
    Add subtour elimination constraints
  end
  Call solver
  Evaluate new subtours
end

Algorithm 4.1: Subtour Elimination Constraint

Listed below is a summary of the constraints with the relevant equation.

Constraint	**Equation**
All heliostats are connected by one incoming and one outgoing cable	(4.2), (4.3)
All heliostats are connected to the receiver tower	(4.4)
All heliostats are continuously connected	(4.4)

Table 4.3: Summary of data cable constraints with the relevant equation numbers; TSP formulation.

4.2.1. Computational Results

After implementing the model in Matlab, the problem was solved with Gurobi on the RWTH compute cluster, which run under the Linux operating system. The calculations were run with 12 cores; a test for parallel speed up over increasing number of cores is described in Section 4.3.2.

The TSP model formulation delivered an optimal result for the cable routing problem, with $n = 624$, within 5.24 hours. To perceive the advantage of this modeling approach, the cost of the cable routing is compared to a naive cable routing approach of the PS10 and also the layout attained by applying the nearest neighbor algorithm. Both results are obtained from the heuristics approach to cable routing in [**?**].

The naive layout is attained by laying the cables in semi-circles around the central receiver tower. To allow for direct comparison, the naive approach was adapted to connect all heliostats with one cable. The Hamiltonian path was calculated with the nearest neighbor algorithm. The 2-opt heuristic was applied to remove any cable crossings [**?**].

Below in Fig. 4.1 the adapted naive approach is displayed, and in comparison the layout attained by the Hamiltonian path and ILP approach as shown in Fig. 4.2 and 4.3.

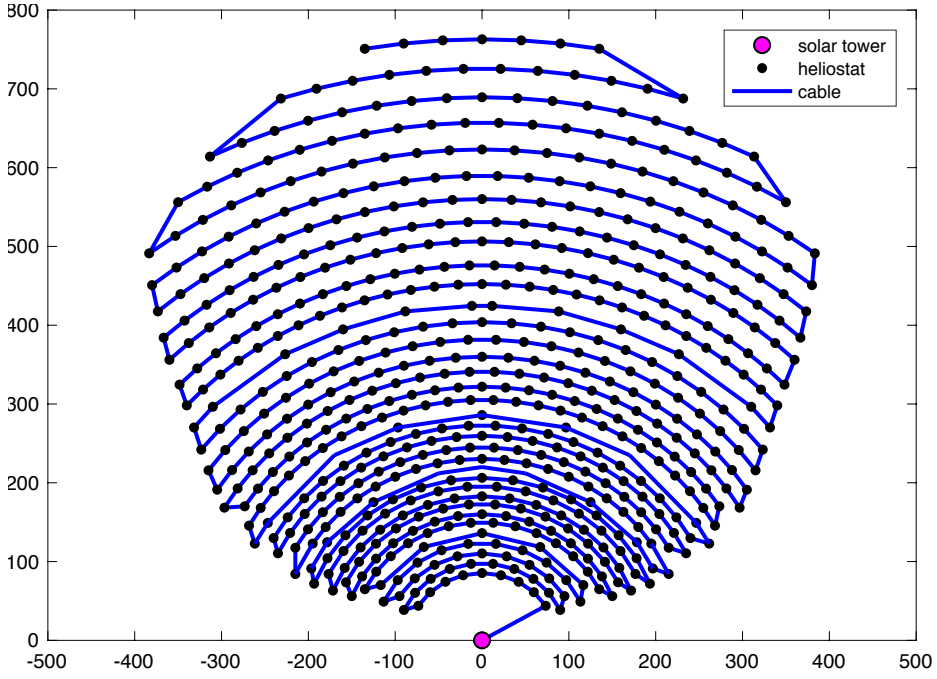

Figure 4.1: Adapted naive layout for the PS10 [**?**]. The cables are installed in semi-circles around the solar tower.
Total cost: 672 511.79 €.

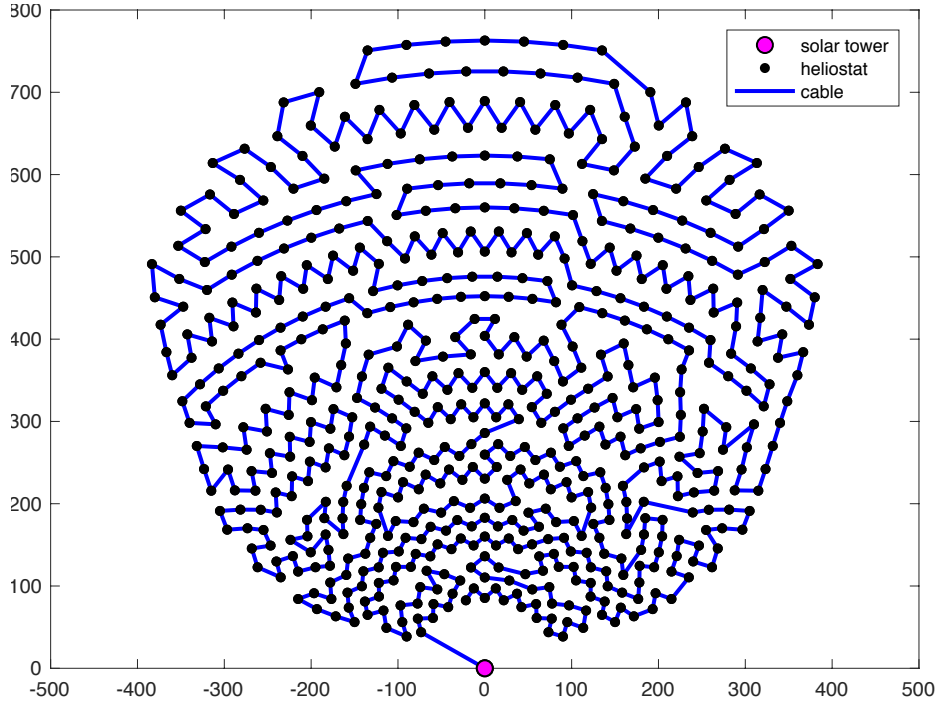

Figure 4.2: Hamiltonian path calculated with nearest neighbor algorithm and 2-opt heuristic [**?**].
Total cost: 548 071.23 €.

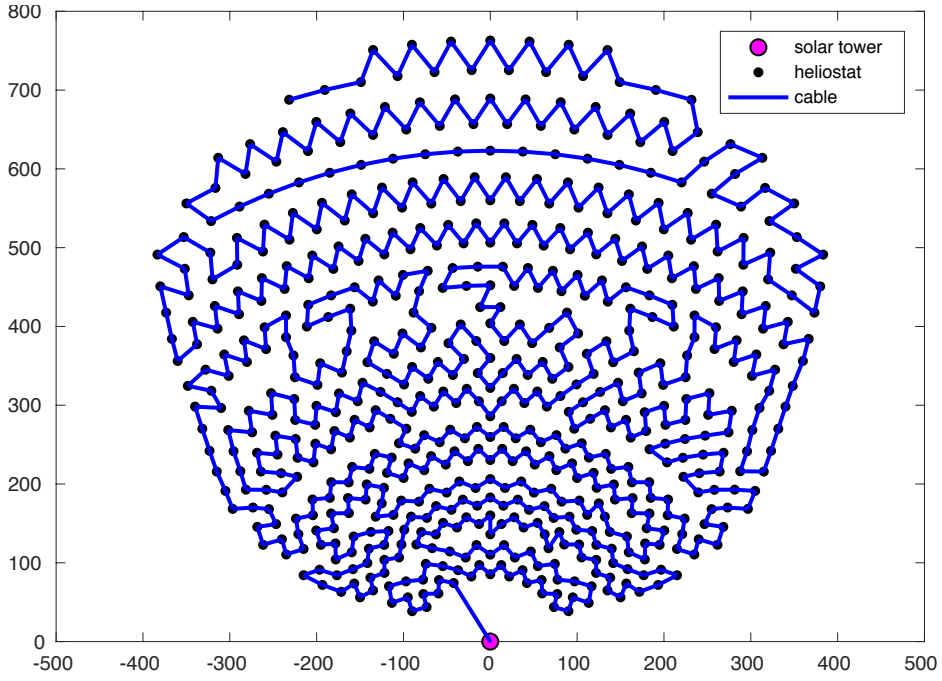

Figure 4.3: Optimal layout of ILP model using exact methods.
Total cost: 534 910.36 €.

The table below presents the total cable meters and total costs resulting from the different approaches. The potential cost savings amount to 22.8 % when compared to the naive layout. This is a result of the cable meter savings, which equal 25.4 %. The Hamiltonian path differs only 2.43 % from the exact solution.

Layout	**Total cable meters** [m]	**Total costs** [€]
Naive	21 038.34	672 511.79
Hamiltonian path	16 747.28	548 071.23
ILP model	16 293.46	534 910.36

Table 4.4: Cable routing comparisons; cost and cable meter savings. Costs calculated for Spain.

In the following bar graph, Fig. 4.4, the different labor costs per country are considered. The cost savings compared to the naive layout amount to 23 %, 24 % and 20.5 % for Spain, Australia and South Africa/UAE respectively. As the labor costs are calculated per meter, the cable meters saved will have a greater impact in Australia than in South Africa/UAE. In a country with lower labor costs, the cost of the switches carry more weight.

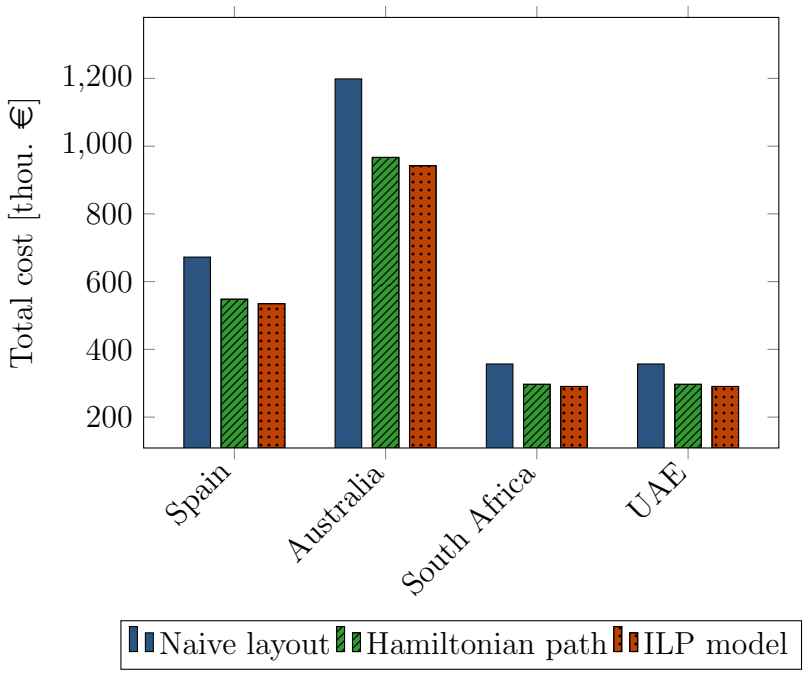

Figure 4.4: Overall costs calculated for Spain, Australia, South Africa and the UAE, under consideration of the varying labor costs.

4.3. Problem Formulation as CVRP

The next approach is to consider a further constraint that limits the maximal attendance number of heliostats per cable connected to the solar tower. This feature is implemented to limit the number of heliostats connected to a single wiring loom. Such a restriction is used in the Shagaya project in Kuwait [**?**]. Consequently, multiple tours, starting from the solar tower, are needed to be able to satisfy the additional restriction. The cable routing formulation can now be described as a VRP or more precisely as a CVRP, restricting the capacity of each tour. The maximal capacity of a tour is referred to by $h_{\max}$. Additionally, the set $\mathcal{X} \subset A$ is defined to contain all edges violating the planarity constraint.

Together with Eq. (4.1), the model reads

$$\sum_{\substack{i \in V \\ i \neq j}} x_{i,j} = 1 \qquad \forall j \in \bar{V} \tag{4.5}$$

$$\sum_{\substack{j \in V \\ i \neq j}} x_{i,j} = 1 \qquad \forall i \in V \tag{4.6}$$

$$\sum_{j \in \bar{V}} x_{1,j} = m \tag{4.7}$$

$$\sum_{\substack{i \in S \\ j \in V \setminus S \\ i \neq j}} x_{i,j} \geq R(S), \quad R(S) = \left\lfloor \frac{|S|}{h_{max}} \right\rfloor \qquad \forall S \subset \bar{V}, S \neq \emptyset \tag{4.8a}$$

$$x_{i,j} + x_{j,i} + x_{k,l} + x_{l,k} \leq 1 \qquad \forall (i,j),(k,l) \in \mathcal{X} \tag{4.9}$$

The constraints (4.5) - (4.6) are the in and out degree constraints of the CVRP formulation; note that they are defined for different sets than in the TSP model. The SEC, defined by Eq. (4.8a), is edited to allow multiple tours, yet none disconnected from the solar tower. The value $R(S)$, is the minimum number of outgoing cables from a violated subtour, so as to adhere to the capacity restrictions. The limited number of connected heliostats $h_{\max}$ is set to 128 in the case of the PS10. With this knowledge, the number of outgoing cables can be set to the fixed value m.

$$m = \left\lceil \frac{n_{heliostats}}{h_{max}} \right\rceil$$

Hence, the number of outgoing cables from the solar tower can be described by Eq. (4.7). Furthermore, to forbid the occurrence of crossings between any of the tours, Eq. (4.9) is implemented and will be referred to as the planarity constraint.

Listed below is a summary of the constraints with the relevant equation.

Constraint	**Equation**
All heliostats are connected by one incoming and one outgoing cable	(4.5), (4.6)
All heliostats are connected to the receiver tower	(4.7), (4.8a)
All heliostats are continuously connected	(4.8a)
Maximum attendance number of heliostats per cable limited to $h_{max} = 128$	(4.8a)
Cable crossings are forbidden	(4.9)

Table 4.5: Summary of data cable constraints with the relevant equation numbers; CVRP formulation.

4.3.1. Planarity Constraint

The final cable routing layout should contain no crossings, due to the higher installation and maintenance costs. Therefore, the occurrence of crossing arcs for one and multiple tours is investigated.

All arcs within a tour adhere to the triangle inequality, described by

$$x_{i,j} \leq x_{i,k} + x_{k,j}$$

this holds for all triples of the vertices i, j, k. A visual example is provided in the following figure,

(a) Connected nodes with crossing edges

(b) Optimal node connections

Figure 4.5: Example of optimal connections within a tour. A shorter route is achieved when no crossings are present.

On the contrary, the optimal solution with two tours starting from the receiver tower could contain crossings. As an example, the following test case was created.

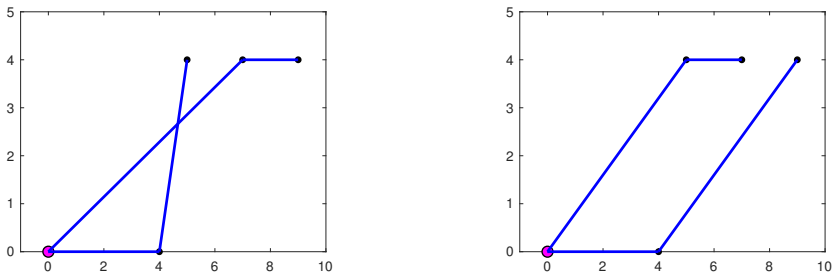

(a) Optimal layout allowing crossings.
Cost: 927.38 €

(b) Layout with planarity constraint.
Cost: 945.38 €

Figure 4.6: Example of crossing edges for multiple routes starting from the depot. Lower costs obtained when crossing is allowed.

As can be seen, the solution containing crossings, results in a cheaper cost compared to the layout in Fig. 4.6b. The layout in Fig 4.6b is obtained after applying the planarity constraint.

The constraint violations are added after the subtour elimination constraint has been called and the dummy edges have been removed. However, calling the planarity constraint after the SEC has been called, might cause violations of the SEC to reoccur. This results in an iterative process between the SEC and the planarity constraint. A detailed flow chart can be found in Fig. 4.7.

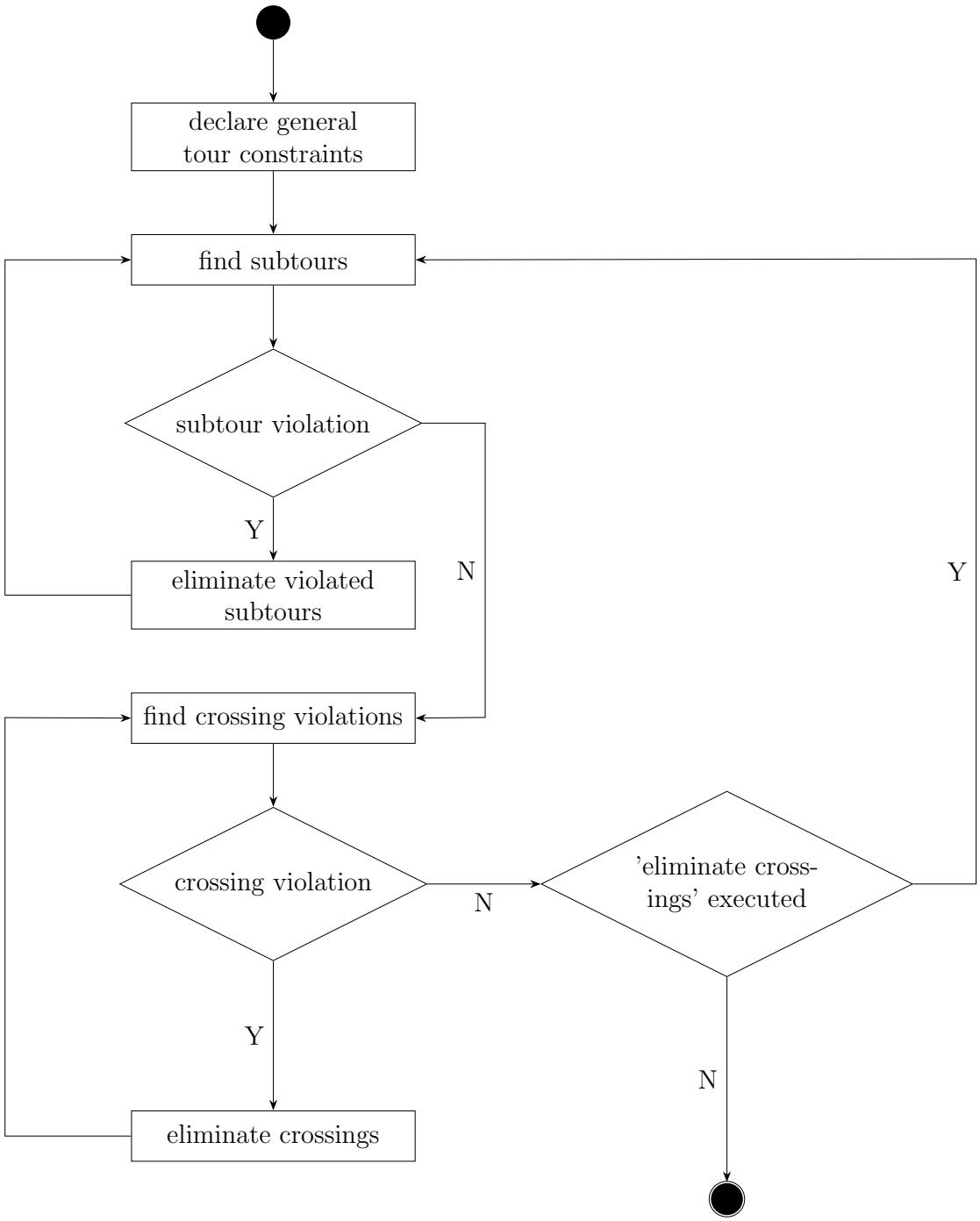

Figure 4.7: Flow chart describing the optimization process of the data cable model. If the planarity constraint is called, a verification of the SEC is needed.

4.3.2. Advantages of Parallelism

The advantage of the Gurobi solver over, e.g. the Matlab solver, is its ability to run in parallel. It is also a vital component when running the optimization solver for large and complex problems. Speedup is defined by,

$$S_p = \frac{T_1}{T_p} \tag{4.10}$$

whereby T_1 denotes the runtime if the calculation is run on one core and T_p the runtime on a multi-core system, p represents the number of cores.

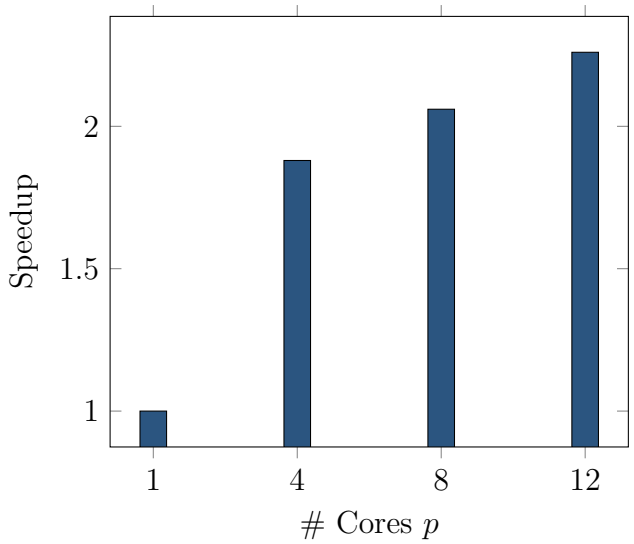

Figure 4.8: Parallel Speedup over cores. Test for $n = 100$ and $m = 2$.

Fig. 4.8 shows the speedup for a varying number of cores. When increasing the number of cores, it is important to remember that for the branch-and-bound tree only the subproblems can be parallelized. The computation time needed at the root node cannot be diminished by increasing the core number. As can be seen, the speedup can be increased to 2.26 for 12 cores. All further calculations will hence be run with 12 cores.

4.3.3. Alternative Subtour Elimination Constraint Formulation

An alternative formulation for the subtour elimination constraint, as discussed by Laporte et al. [**?**], is defined by,

$$\sum_{\substack{i,j \in S \\ i \neq j}} x_{i,j} \leq |S| - R(S) \qquad \forall S \subset \bar{V}, S \neq \emptyset. \tag{4.8b}$$

Eq. (4.8b), ensures that within the subtour the number of connections is diminished, and therefore referred to as inner connectivity constraint (ICC). The constraint defined in Eq. (4.8a) ensures that the subtour violating the constraint has $R(S)$ connections to all other nodes in the field, and will from now on be referred to as the outer connectivity constraint (OCC). As discussed in [**?**], these formulations are mathematically equivalent. However, as found in [**?**], the formulations can lead to different ILP-solver performances. For an increasing number of nodes (heliostats), the runtimes of formulation OCC and ICC are compared. The number of tours was set to two.

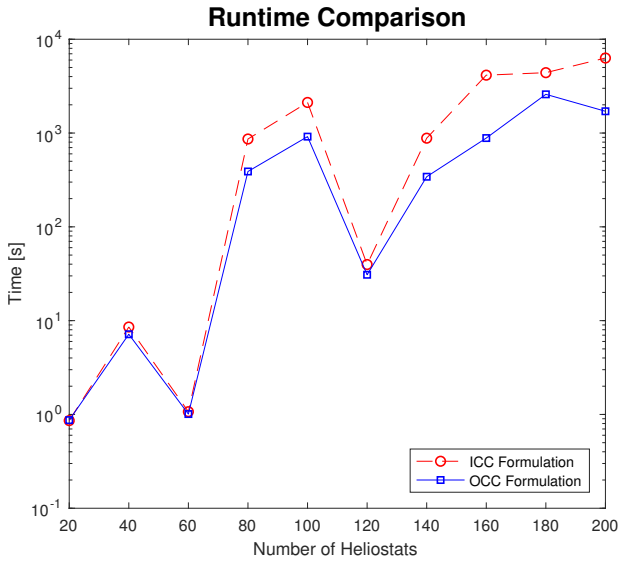

Figure 4.9: Runtimes for subtour formulations OCC and ICC with $m = 2$. The OCC formulations results in a reduced runtime.

As can be seen in Fig. 4.9 the OCC formulation performs better overall. The deviations at 60 and 120 as well as 80 and 100 heliostats is owed to the presolve and heuristic methods used by the solver. If the methods deliver a very good incumbent value early on, only a few iterations are needed to find the true optimal solution. If, however, a good incumbent value is not easily found or not close to the best bound, more iterations are needed at the cost of an increased runtime.

4.3.4. Optimization using a Start Value

Speedup of the optimization process is often achieved by limiting the size of the branch-and-bound tree [**?**]. By presenting the solver with a start value, a smaller gap between the incumbent and best bound can be found early on during the optimization process. It can however, make no difference at all, if the Gurobi heuristic methods find a value that is just as good or better than the start value.

The effect of providing a start value is tested for both subtour elimination formulations and for a varying number of heliostats. The start value is obtained from the heuristics

approach used in [**?**]. During this approach, the best result was achieved by use of a Hamiltonian path. Note that the runtimes with a start value do not include the time needed to calculate the start value itself.

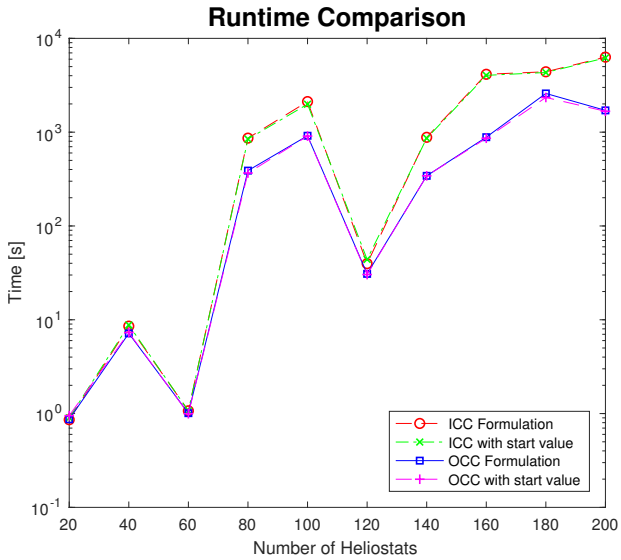

Figure 4.10: Runtimes including and excluding start values for subtour formulations OCC and ICC. No benefit was achieved by including a start value.

Fig. 4.10 shows that providing a start value did not benefit the runtime. The OCC formulation still delivers better runtimes and barely any discrepancy between the runs including and excluding a start value can be seen. The reason behind this can be explained by looking at the incumbent values and relative gap.

Looking closer at the 200 heliostat test, the incumbent value differs no more than 0.41 % from the best bound (when the solver is called for the first time). The first two subplots in Fig. 4.11 depict the incumbent values and the best bound for the cases with and without a start value. Without the start value the required gap tolerance is reached within four seconds. Furthermore, it can be seen that within two seconds a relative gap of less than 0.01 % is achieved for the case not including a start value. While the case including a start value has a relative gap of less than 0.001 %, the time needed to reach a gap tolerance of $10e^{-10}$ remains the same for both cases. This also explains why the runtimes differ only in the slightest. Even though the solver is called multiple times, the time saved remains negligible.

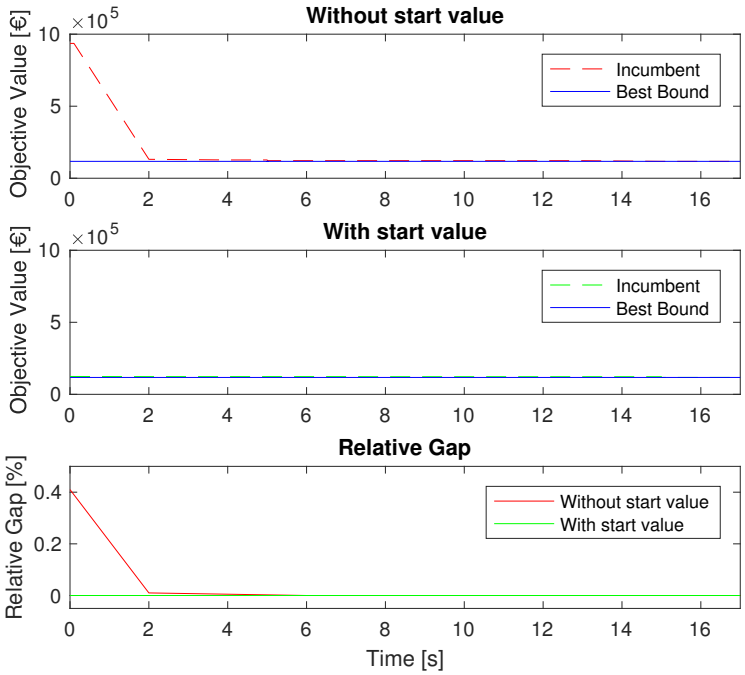

Figure 4.11: Relative gap including and excluding a start values. Calculations without a start value achieve the same gap tolerance value within 2 seconds.

4.4. Runtime Limitations

Steadily increasing the problem size, proved to immensely affect the runtime. The goal, however, is to run the CRVP model for the PS10 with five tours, therewith adhering to the capacity constraints. To which extent multiple tours affect the runtime is therefore tested. The tests were run to find the maximal heliostat number that can be optimized within an acceptable amount of time.

Creating only one tour, it was possible to solve to optimality within 5.24 hours. For this case a single fiberglass cable is installed, connecting all 624 heliostats. Hence, the next calculations were all restricted to a 6h runtime limit, in order to compare the impact of multiple tours on the runtime. Again all calculations were run with twelve cores and the OCC subtour formulation was used. The calculations were run for one, two, three, four and five tours.

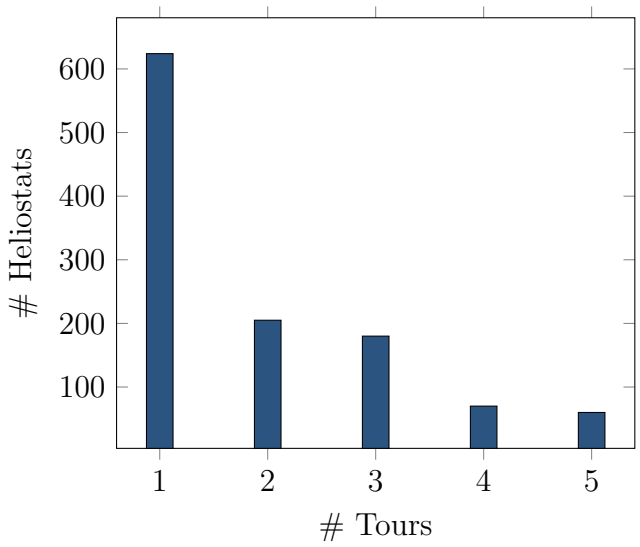

Figure 4.12: Maximal heliostat optimization within 6 h. For 5 tours, the problem could be solved for $n = 60$.

For two tours, the amount of heliostats is a third of the TSP model. Reaching five tours, the number is reduced to 60 heliostats, which is a tenth of the size of the PS10.

4.4.1. CVRP Formulation for PS10

Limiting factors are not only confined to the runtime, but memory usage limitations need to be considered as a restraint factor as well. On the one hand, the constraint matrices became extremely large in size, as with each subtour violation a new constraint is added. Additionally, with limited resources available, a restart functionality had to be added to the program. As a result, the large matrices and other variables would always have to be stored and loaded after and before every restart of the calculation. Conclusively, after 343 h the layout still contained violated subtours. This can be seen in Fig. 4.13.

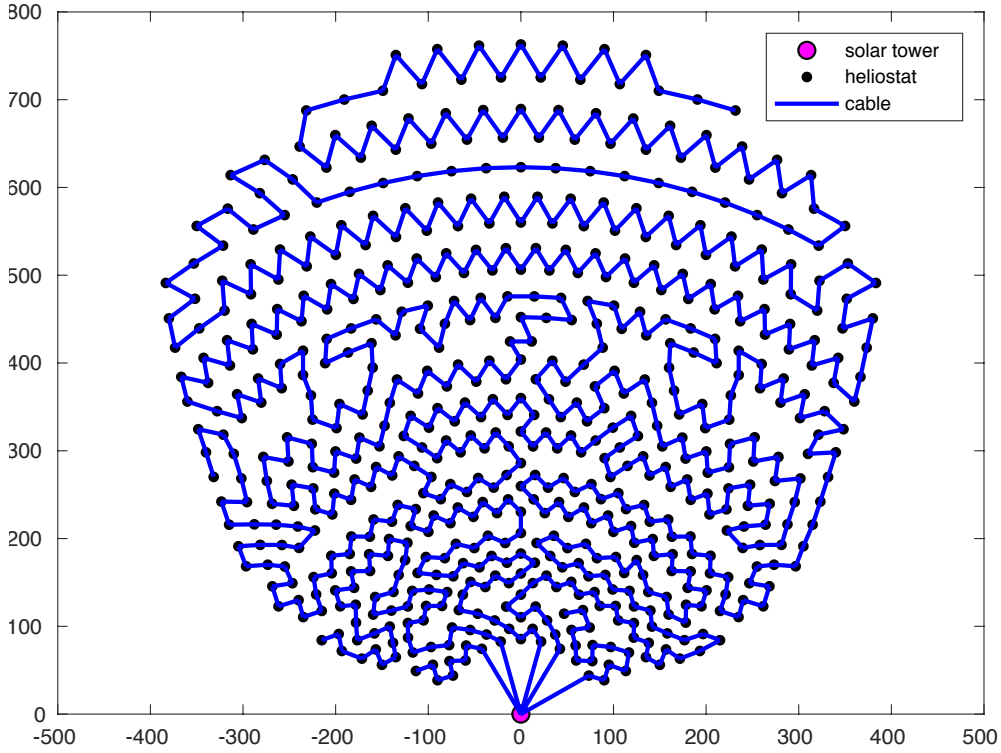

Figure 4.13: CVRP formulation of PS10 with $m = 5$ and $n = 624$. Layout still contains subtour constraint violations. Runtime 381 h.

4.5. Result Evaluation and Conclusion

The entire PS10 with five tours did not provide a solution in a practical amount of time, consequently, the problem size was reduced to 60 heliostats for five tours. In doing this, it is possible to validate the heuristic methods used in [**?**] for small problem sizes. The cable meters used differed 5.94 %, resulting in a cost difference of 5.24 %.

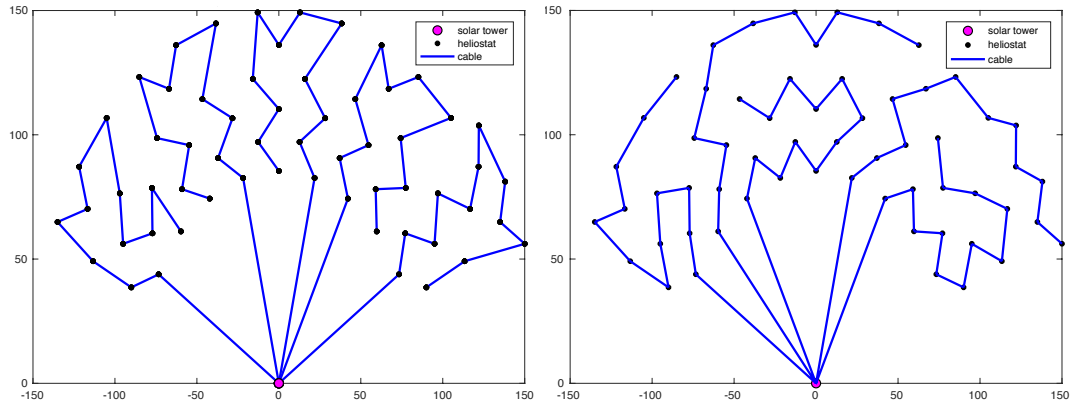

(a) Hamiltonian path calculated with nearest neighbor algorithm and 2-opt heuristic, cf. [**?**]

(b) Optimal layout for CVRP formulation using exact method.

Figure 4.14: Cable routing comparison for $n = 60$ and $m = 5$.
Cost difference 5.24 %.

Comparing the results for a medium problem size of 200 heliostats, two tours are used, as this has been shown to complete within realistic time limits.

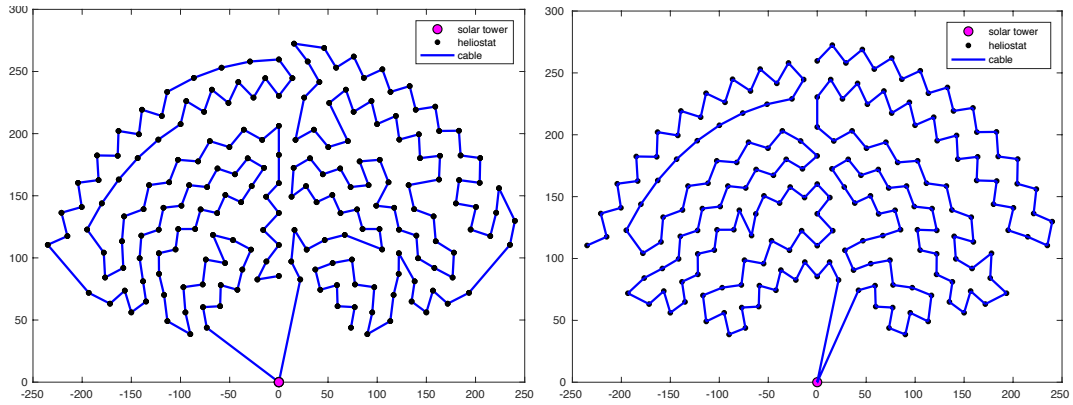

(a) Hamiltonian path calculated with nearest neighbor algorithm and 2-opt heuristic, cf. [**?**]

(b) Optimal layout with ILP model using CVRP formulation

Figure 4.15: Cable routing comparison for $n = 200$ and $m = 2$.
Cost difference 4.57 %.

The medium sized instance resulted in a cable meter disparity of 5.33 % and a cost difference of 4.57 %.

Referring back to Section 4.2.1, the cable meters reduced by 2.75 % for the ILP model compared to the heuristic method, proceeding to differ 2.43 % in the overall costs.

The complexity of the model is greatly affected by the addition of multiple tours. Therefore, if no restrictions on the maximal cable length or number of heliostats connected is needed, the ILP model can optimally solve the cable routing problem for 624 heliostats within an acceptable amount of time. If however, these restrictions are in place, a different approach is worth considering. The runtime for the PS10, restricting the connected heliostats to 128, exceeds practical applications.

The cost difference between the heuristic and exact method remain around 5 % for the small and medium problem sizes. It is therefore plausible, to use the heuristic methods to obtain a good estimate cost for the cable layout.

Taking a closer look at the solution obtained by the exact method for the 200 heliostats, the layout results in similar partitioning of the routes. It therefore might be worth relaxing the problem and implement predefined sections, which could be solved independently. This would allow for a solution of the entire PS10 with five tours.

5. Power Cable Model

The power cable model has additional constraints which were not present in the data cable model. Therefore, the power cable is described by the distance and capacity constrained VRP, as explained in Section 5.1. The necessary capacity restrictions are added to the model in Section 5.2.1, while in Section 5.2.3 the model is extended to include the length restrictions.

5.1. Modeling Approach

Since it has to be assure that the current flowing through the cable does not surpass its capacity, the capacity and length restrictions are implemented. With the additional constraints in place, it is no longer possible to model the cable routing problem as a TSP, as this would require cables of unrealistic cross sections. Hence, a model is required that adheres to both the capacity and length restriction, under consideration of the available cable types. Accordingly, the cable routing problem is modeled as a distance and capacity constrained VRP (DCVRP). An overview of the required constraints is shown in Table 5.1.

Formulation	**Constraint**	**Cost model**
DCVRP	• All heliostats are connected to the receiver tower • All heliostats are connected by one incoming and one outgoing cable • Cable crossings are forbidden • All heliostats are continuously connected with the maximum number of heliostats per cable type defined by h^t • The length of cable type t is restricted to a maximum length of l^t	• Cable types of different capacities are considered • Consideration of installation costs, i.e. protective foil and labor costs

Table 5.1: Overview of power cable constraints and cost model.

5.1.1. Miller-Tucker-Zemlin Formulation

For the power cable model, the Miller-Tucker-Zemlin (MTZ) formulation will be used. The advantage of this formulation is the relatively simple generalization of other VRP constraints. Although the CVRP can be modeled with the classical subtour elimination constraints, an extension to the distance constrained VRP is not so easily achieved. A DCVRP can therefore be more easily modeled with the MTZ formulation, also extendable to route specific constraints. Still, a known disadvantage is the weak LP relaxation produced by the MTZ formulation [**?**].

The MTZ constraints replace the SEC used for the data cable implementation. The number of added constraints is reduced to $\mathcal{O}(n^2)$ for a problem size containing n customers, however with the addition of flow variables u_i. This is an advantage over the possibly exponential number of constraints needed for the SEC formulation, with $\mathcal{O}(2^n)$ [**?**].

The generalized MTZ formulation reads,

$$u_i - u_j + Mx_{i,j} \leq M - q_j \qquad \forall i, j \in V \tag{5.1}$$

with u_i representing the accumulated demand at node i, M is an arbitrarily large value, having the effect that if $x_{i,j} = 0$ the inequality becomes inactive, and q_j is the demand at node j. No disconnected tours from the depot are possible, as this would lead to a contradiction in the formulation. [**?**]

5.2. Problem Formulation as a DCVRP

A digraph G is considered with $\bar{V}$ representing the heliostats in the field and the set V representing the heliostats and the solar tower. In addition, the set T is defined, which contains all available cable types t, whereby $t = 1$ defines the cable of lowest capacity and $t = k$ the cable of highest capacity. The capacity and length constraints need to be applied to each route, hence the need to define set R, which contains all routes $r = \underline{m}, ...\overline{m}$. Furthermore, let m be a free variable and denote the number of outgoing cables from the solar tower. The lower bound on the variable m is determined by,

$$\underline{m} = \left\lfloor \frac{n_{heliostats}}{t_k} \right\rfloor,$$

while the upper bound is defined by,

$$\overline{m} = n_{heliostats}.$$

As the capacity and length restrictions need to be applied to each route individually, artificial depots are included in the model, which will be removed again at the end

of the optimization process. The number of artificial depots equals $\overline{m} - 1$, which increases the number of nodes to $n' = n + \overline{m} - 1$. Thereby, the extended set is defined as $V' = 1, ...n'$ and $\bar{V}' = V' \setminus \{1\}$.

The inclusion of multiple cable types in the formulation, results in the cost matrix,

$$\begin{aligned} \tilde{c}_{i,j}^t &= d_{i,j} \cdot \bar{c}^t \\ \text{with} \quad \bar{c}^t &= \check{c}_{cable}^t + c_{labor}, \end{aligned}$$

with,

$$\tilde{c}_{i,j}^t = \begin{cases} \tilde{c}_{i,j}^t & \forall i \in V', j \in \bar{V}' \text{ and } i \neq j \\ \tilde{c}_{i,j}^t = \hat{M} & \forall i \in V' \setminus V, i \in \bar{V}', i \neq j \\ \tilde{c}_{i,j}^t, \tilde{c}_{j,i}^t = M & \forall i \in V' \setminus V, j \in V' \setminus V, i \neq j \\ \tilde{c}_{i,1}^t = \hat{M} & \forall i \in \bar{V}, i \neq j, \\ \tilde{c}_{i,1}^t = 0 & \forall i \in V' \setminus V, i \neq j, \end{cases} \tag{5.2}$$

whereby $\hat{M} > M \in \mathbb{R}$. The definitions in Eq. 5.2 assure that firstly, an artificial depot is not connected to another artificial depot. Secondly, the connection between nodes is preferred over connections between a node and artificial depot. And lastly, the edge returning to the solar tower will always be connected to an artificial depot, meaning that an artificial depot will always be the last node visited during a tour. The assignments are necessary, so that the layout of the cable is not affected by the introduction of the artificial depots.

Now, let $x_{i,j}^t, (i \neq j)$ be a binary variable with,

$$x_{i,j}^t = \begin{cases} 1 & \text{if heliostat } i \text{ is connected to heliosat } j \text{ with cable type } t \\ 0 & \text{otherwise.} \end{cases}$$

Also, let $x_{i,j,r}^t, (i \neq j)$ be a binary variable with,

$$x_{i,j,r}^t = \begin{cases} 1 & \text{if heliostat } i \text{ is connected to heliosat } j \text{ with cable type } t \text{ and belongs to route } r \\ 0 & \text{otherwise.} \end{cases}$$

Hence, the power cable model reads,

$$\min \sum_{\substack{i,j \in V' \\ i \neq j}} \sum_{t \in T} \tilde{c}_{i,j}^t \cdot x_{i,j}^t \tag{5.3}$$

$$\text{s.t.} \sum_{i \in V'} \sum_{r \in R} \sum_{t \in T} x_{i,j,r}^{t} = 1 \qquad \forall j \in \bar{V}' \tag{5.4}$$

$$\sum_{j \in \bar{V}'} \sum_{r \in R} \sum_{t \in T} x_{i,j,r}^{t} = 1 \qquad \forall i \in V' \tag{5.5}$$

$$\sum_{j \in \bar{V}'} \sum_{r \in R} \sum_{t \in T} x_{1,j,r}^{t} \geq \underline{m} \tag{5.6}$$

$$\sum_{i \in V'} \sum_{t \in T} x_{i,l,r}^{t} - \sum_{j \in V'} \sum_{t \in T} x_{l,j,r}^{t} = 0 \qquad \forall l \in V', r \in R \tag{5.7}$$

$$\sum_{r \in T} x_{i,j,r}^{t} = x_{i,j}^{t} \qquad \forall i, j \in V', t \in T \tag{5.8}$$

$$\sum_{t \in T} x_{i,j}^{t} + x_{j,i}^{t} + x_{u,v}^{t} + x_{v,u}^{t} \leq 1 \qquad \forall (i,j), (u,v) \in \mathcal{X} \tag{5.9}$$

$$x_{i,j}^{t} \in \{0,1\} \tag{5.10}$$

$$x_{i,j,r}^{t} \in \{0,1\} \tag{5.11}$$

$$\underline{m} \leq m \leq \overline{m}, \in \mathbb{Z}^{+}. \tag{5.12}$$

Constraints (5.4) and (5.5) are the degree constraints. The number of outgoing cables from the solar tower is restricted by Eq. (5.6). The variable m is free, and can be restricted by the definition in (5.12). The variable m is not fixed, as the optimal layout could be to introduce more tours and therewith using more of the cheaper cable types. On the contrary, the optimal solution might include less but therefore larger tours utilizing higher capacity and so with more expensive cable types. Furthermore, Eq. (5.7) is the connectivity constraint, while Eq. (5.8) defines the variable $x_{i,j}^{t}$. Eq. (5.9) forbids the formation of cable crossings and is comparable to the planarity constraint implemented in the data cable model.

5.2.1. Capacity Restrictions

The additional variables, present in the MTZ formulation of the capacity constraints, read $q_{i,r}, \forall i \in V'$, $q_{o,r}, \forall i \in V'$ and $p_j, \forall j \in \bar{V}'$. The variables describe the accumulated demand at node i and the demand at the artificial node, respectively. The variable p_j defines the demand at the node j and can in this case be set to $p_j = 1$. The variable Q is equal to the capacity of the largest cable type.

A further binary variable, $y_{i,r}$ is introduced, defined by,

$$y_{i,r} = \begin{cases} 1 & \text{if heliostat } i \text{ is visited by route } r \\ 0 & \text{otherwise.} \end{cases}$$

Forthwith, alongside the constraints (5.4) - (5.9), the model reads,

$$Q - p_j \geq \sum_{r \in R}(q_{i,r} - q_{j,r} + \sum_{t \in T} Q \cdot x^t_{i,j,r}) \qquad \forall i \in V', j \in \bar{V}' \qquad (5.13)$$

$$\sum_{i \in V'} \sum_{t \in T} x^t_{i,j,r} = y_{i,r} \qquad \forall j \in V', r \in R \qquad (5.14)$$

$$\sum_{j \in V'} \sum_{t \in T} h^t \cdot x^t_{i,j,r} \geq q_{o,r} - q_{i,r} - M \cdot (1 - y_{i,r}) \qquad \forall i \in \bar{V}', r \in R \qquad (5.15)$$

$$\sum_{i \in V'} q_{i,r} = q_{o,r} \qquad \forall r \in R \qquad (5.16)$$

$$2 \cdot y_{i,r} \leq q_{i,r} \leq Q \cdot y_{i,r} \qquad \forall i \in \bar{V}', r \in R \qquad (5.17)$$

$$q_{i,r}, q_{o,r}, p_j \in \mathbb{Z}^+ \qquad (5.18)$$

$$y_{i,r} \in \{0, 1\} \qquad (5.19)$$

$$x^t_{i,j} \in \{0, 1\} \qquad (5.20)$$

$$x^t_{i,j,r} \in \{0, 1\}. \qquad (5.21)$$

The capacity of a tour is restricted by Eq. (5.13), which also serves to avoid subtours. The variable $y_{i,r}$ is defined by Eq. (5.14), while the variable $q_{o,r}$ is defined by Eq. (5.16). Eq. (5.15) are the cable type specific capacity constraints and enforce the capacity restriction for each cable type t. Lastly, Eq. (5.17) defines the limits of the variable $q_{i,r}$

A visual clarification of the cable type specific capacity constraints is shown in Fig 5.1. The constraint assures that the cable leaving the solar tower is able to withstand the current flow of all succeeding heliostats connected to the same cable.

5.2.2. Computational Results with Capacity Constraints

The CVRP formulation is applied to test cases with 10 heliostats. The different cable types are adjusted to suit the smaller test cases. The cable type capacities are defined

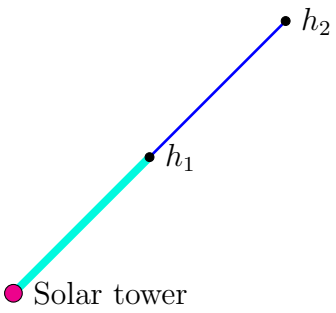

Figure 5.1: The cyan (thick) cable needs to withstand current flow of heliostat h_1 and h_2. The blue (thin) cable needs to withstand current flow of h_2 only.

in the table below.

Cable Type t	**Color in plot**	**Test case 1: Capacity** h^t**.**	**Test case 2: Capacity** h^t**.**
1		5	1
2		10	3
3			10

Table 5.2: Example cable type capacities and definition of colors used to present cable type in the plot.

The first test case, depicted in Fig. 5.2, shows the connection of ten heliostats with two available cable types. The optimized layout uses both cable types instead of creating two tours.

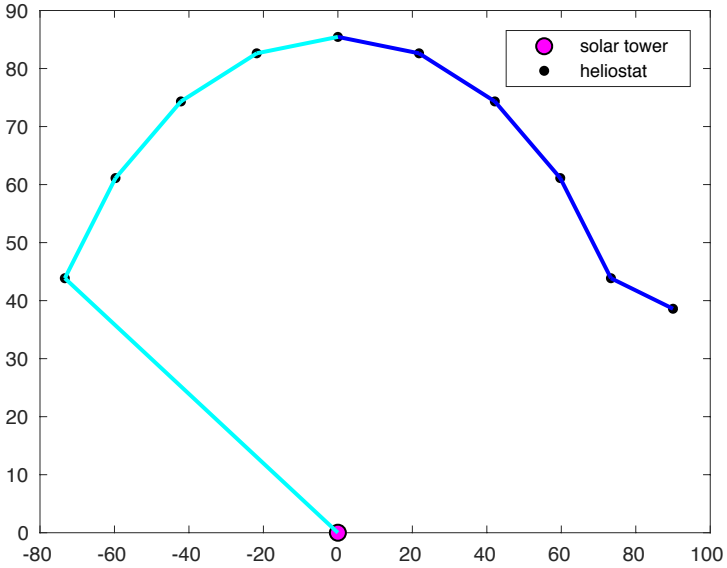

Figure 5.2: Optimized cable layout with two available cable types.

For the second test case, another cable type was made available and cable types $t = 1$ and $t = 2$ restricted to a capacity of 1 and 3 heliostats respectively. Again, the optimized layout contains only one tour.

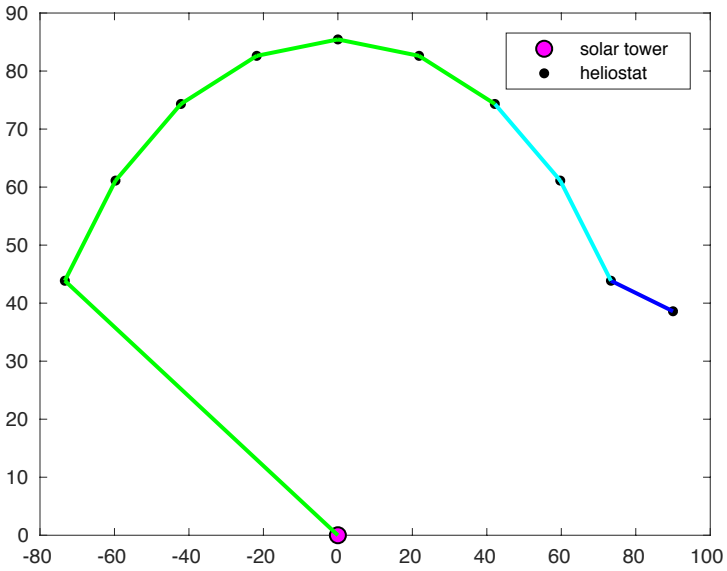

Figure 5.3: Optimized cable layout with three available cable types.

For small instances of the problem, the optimal layout contains less tours making use of more expensive cable types. This is a result of the initial connection from the solar tower to the first heliostat on the route. With multiple tours, the total cable length increases which outweighs the benefit of using cheaper cable types.

5.2.3. Length Restrictions

A further constraint pertaining to the length restriction of each cable type still needs to be considered for the model. A complication lies in the optimization of the length of each cable type. As shown in the equation below, the length is dependent on the number of heliostats connected. The greater the current flowing through a cable, the shorter the allowable length. The length is defined by,

$$l_t = \frac{q_t \cdot \kappa \cdot dU \cdot U \cdot cos(\phi)}{2 \cdot P \cdot h^t} \tag{5.22}$$

where q_t is the cross section of each cable type, κ the electrical conductivity of copper, U represents the voltage and dU the voltage drop. Lastly, $cos(\phi)$ defines the power factor, P the power of the alignment motor and h^t the number of connected heliostats.

The idea would be to optimize the tour length under consideration of the available cable types. Optimally, a maximum number of heliostats over a maximum total distance are connected, bearing in mind the trade off between cable length and number of heliostats.

Defining MTZ constraints for the length constraints, the following variables are introduced. The accumulated length at each heliostat is denoted by $g_{i,r}, \forall i \in \bar{V}, r \in R$. The variable s_i refers to the minimum distance between the solar tower and any heliostats in the field. It presents the lower bound for the variable $g_{i,r}$. The maximal length L per route is defined by the sum of all l_t.

Alongside Eq. (5.3) - (5.17), the model reads,

$$L - d_{i,j} \geq \sum_{r \in R}(g_{i,r} - g_{j,r} + \sum_{t \in T} L \cdot x^t_{i,j,r}) \qquad \forall i \in V', j \in \bar{V}' \tag{5.23}$$

$$\sum_{i \in V'} \sum_{t \in T} x^t_{i,j,r} \cdot \tilde{l}^z \geq g_{o,r} - g_{i,r} - M \cdot (1 - y_{i,r}) \qquad \forall j \in V', r \in R \tag{5.24}$$

$$\sum_{i,j \in V} d_{i,j} x^t_{i,j,r} \leq l_t \qquad \forall t \in T, r \in R \tag{5.25}$$

$$\sum_{i \in V'} g_{i,r} = g_{o,r} \qquad \forall r \in R \tag{5.26}$$

$$s_i \cdot y_{i,r} \leq g_{i,r} \leq L \cdot y_{i,r} \qquad \forall i \in \bar{V}', r \in R \tag{5.27}$$

$$g_{i,r}, g_{o,r} \in \mathbb{Q}^+ \tag{5.28}$$

$$y_{i,r} \in \{0, 1\} \tag{5.29}$$

$$x_{i,j}^{t} \in \{0,1\} \tag{5.30}$$

$$x_{i,j,r}^{t} \in \{0,1\}. \tag{5.31}$$

The Eq. (5.23) restricts the total length for each tour, while (5.24) and Eq. (5.25) refer to the length restriction of each cable type within a tour. The limits of $g_{i,r}$ are defined by Eq. (5.27). Again, Eq. (5.26) defines the variable $q_{o,r}$

Note that

$$\tilde{l}^{z} = \sum_{t=1}^{z} l^{t} \qquad \forall z \in T.$$

An example of the length restriction per cable type is given in Fig. 5.4.

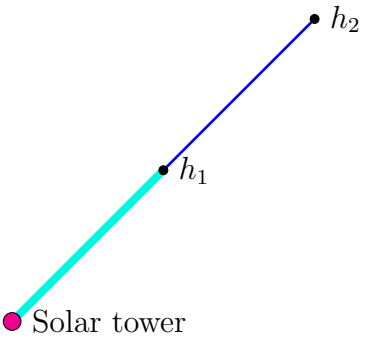

(a) Length restriction for only two succeeding heliostats.

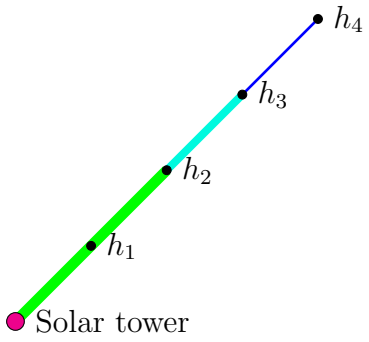

(b) Length is reduced as a result of additional heliostats connected by the same cable.

Figure 5.4: Example of the length restriction. With additional heliostats, the length of the blue and cyan colored cable type is reduced.

In the first example, Fig. 5.4a, only two heliostats are connected by the same cable. However, if additional heliostats are added, the allowable length for the blue and cyan colored cable type are reduced. The cable now has to withstand the current flow of four heliostats, as apposed to two earlier. A further cable type might therefore have to be introduced, to connect the remaining heliostats.

5.3. Conclusion

A recapitulation of all constraints need for the power cable model can be found in Appendix C. A review of the constraints an their equations is described in the following table,
A capacitated VRP model was described and tested for small test cases. The optimal route includes the consideration of best cable type to use with regard to the capacity

Constraint	**Equation**
All heliostats are connected to the receiver tower	(5.13), (5.23)
All heliostats are connected by one incoming and one outgoing cable	(5.4) , (5.5)
Cable crossings are forbidden	(5.9)
All heliostats are continuously connected with the maximum number of heliostats per cable type defined by h^t	(5.15)
The length of cable type t is restricted to a maximum length l^t	(5.24), (5.25)

Table 5.3: Summary of power cable constraints with the relevant equation numbers.

constraints. An extensive model is given for the combined capacity and length constrained model. Due to the excessive runtime, these are not expanded on here. An approximative approach is described in Appendix B.

6. Concluding Remarks

A short summary of the achieved results will be given in the following section and some recommendations for future work will be given in Section 6.2.

6.1. Conclusion

The TSP model approach for the data cable model can be deemed successful for the PS10. By modeling the cable routing problem as a TSP, only LOCs of type conductor are needed. This however, falls back on the assumption that one cable can connect all 624 heliostats. In terms of maintenance, this approach could be problematic. If, e.g. a fault in the cable occurs near the solar tower, the remaining part of the field will be affected as well.

The data cable model approach as a CVRP can be used to validate heuristic methods for small to medium problem sizes. Again, only conductor switches are needed in the layout, providing an advantage over a minimum spanning tree layout for example. Using exact methods to solve the capacitated VRP for larger sized models, such as the PS10, is impractical due to the overlong runtime.

The heuristic models for the data cable differed around only 5 % from the exact model, confirming the plausibility of the results obtained by heuristic methods. It also confirms the benefit of optimizing the cable routing of solar tower plants.

The capacity constraints of the power cable were successfully implemented. As a result the layout includes the choice of the best cable type under consideration of the capacity restrictions. The length restriction per cable type was described theoretically only, due to runtime limitations.
Overall, it was possible to model the data cable and the capacity constraints of the power cable as integer linear programs and obtain computational results confirming the model formulations.

6.2. Outlook

The need for further research was emphasized in Section 4.4 and again in Section 5. The goal ultimately should be to run the exact optimization for large fields of sizes ranging around 12 000 heliostats., such as the planned solar tower power in South Africa, the Redstone Solar Thermal Power Plant.

Looking at the currently implemented formulations, it could be worthwhile strengthening the subtour elimination constraints for the data cable. The runtime is predominantly spent on the SEC. At present, subtours only violate the SEC if the tour is either too large or disconnected from the solar tower. A further violation could include the

minimum length of a subtour.

In terms of the power cable model, the current inequalities could be strengthened similar to the described proceedings in [**?**]. A further modeling approach can be considered which allows branching at the heliostats. Branching does not incur additional costs, as no additional electrical elements, such as switches, are needed.

Another cost saving factor would be to consider the power and data cable as one. This approach will reduce the labor costs, which are still the most expensive component of the cost model. However, optimizing both cables as one will further complicate the model, as the collective constraints increase the model size.

Conclusively however, using exact methods alone will most likely not deliver a result in an acceptable amount of time, if at all. Therefore, it is important to look at other options, such as introducing relaxations of the model.

An example of a relaxation could be to cluster the heliostats into groups and then optimize each group locally. Whereby the problem arises of choosing the correct cluster size and locations of the clusters. Furthermore, a STP field is normally structured into a radially staggered grid, where it might be possible to use this structure as an advantage. Lastly, it could be worth installing a distribution box in the center of the field, meaning that only one cable needs to cover the distance from the solar tower to the heliostat field.

All in all, researching the optimized cable routing layout of solar tower power plants has already shown to provide large cost saving benefits and should therefore be researched further and later adopted when constructing STPs.

A. Power Cable Calculations

The current I can be calculated by

$$I = \frac{P}{U \cdot cos(\phi) \cdot \eta} \tag{A.1}$$

where P defines the power of the alignment motor, U the voltage, $cos(\phi)$ the power factor and η the energy conversion efficiency.
Eq. (A.1) can then be used to calculate the maximum number of heliostats k connected to a cable of type t.

$$r_i \cdot R_{max} \overset{!}{\leq} \frac{k \cdot P}{U \cdot cos(\phi) \cdot \eta}$$

$$\Leftrightarrow \quad k = \left\lfloor \frac{r_i \cdot R_{max} \cdot U \cdot cos(\phi) \cdot \eta}{P} \right\rfloor \tag{A.2}$$

In this case r_t is the current rating and R_{max} the maximal current rating. The current ratings can be found in [**?**] for an assumed constant temperature of 20°C at a minimum of 0.8m below ground level. R_{max} determines to what capacity the cables are exposed. R_{max} is set to 80%, keeping a reserve of 20%.

	Parameter	**Selected value**
Voltage	U	230V
Voltage drop	dU	6%
Power of alignment motor	P_{motor}	100W
Power factor	$cos(\phi)$	0.95
Energy conversion efficiency	η	0.9
Electrical conductivity of copper	κ	57 $\frac{m}{\Omega \cdot mm^2}$
Utilization of maximal current rating	R_{max}	80%

Table A.1: Overview and description of the parameters used to calculate the capacity and length restrictions.

B. Power Cable Length Approximation

The complexity of the length restriction can be reduced by adopting an approximative approach. Regard δ_{min} to define the minimum distance between all heliostats in the field. In case of the PS10, the minimum distance equals

$$\delta_{min} = 16.5393\text{m}$$

For all cable types, find a distance that conforms with

$$l \geq n \cdot \delta_{i,j}$$

These values have been calculated for each cable type,

Cable type	**Maximal length** [m]	**Cable capacity** h^t
1	181.93	11
2	231.55	14
3	281.17	17
4	363.86	22
5	463.10	28
6	595.41	36
7	694.65	42

Table B.1: Maximal cable length and capacity restriction for each cable type.

Hence, instead of a length that is dependent on the number of heliostats connected, a maximum length for each cable type has been calculated and can be implemented in the same way as the capacity constraint.

As it is possible, that the total length will not have been fully exploited, a post-processing step should be introduced. This evaluates if a further heliostat can be connected with a cheaper cable type, without violating the capacity or length constraints. The post-processing would only change the cable type used and keep the layout as is.

C. Recapitulation of All Power Cable Constraints

For an overview of the constraints needed for the power cable model, the complete model reads,

$$\min \sum_{\substack{i,j\in V' \\ i\neq j}} \sum_{t\in T} \tilde{c}^t_{i,j} \cdot x^t_{i,j} \tag{C.1}$$

$$\text{s.t.} \sum_{i\in V'} \sum_{r\in R} \sum_{t\in T} x^t_{i,j,r} = 1 \qquad \forall j \in \bar{V}' \tag{C.2}$$

$$\sum_{j\in \bar{V}'} \sum_{r\in R} \sum_{t\in T} x^t_{i,j,r} = 1 \qquad \forall i \in V' \tag{C.3}$$

$$\sum_{j\in \bar{V}'} \sum_{r\in R} \sum_{t\in T} x^t_{1,j,r} \geq \underline{m} \tag{C.4}$$

$$\sum_{i\in V'} \sum_{t\in T} x^t_{i,l,r} - \sum_{j\in V'} \sum_{t\in T} x^t_{l,j,r} = 0 \qquad \forall l \in V', r \in R \tag{C.5}$$

$$\sum_{r\in T} x^t_{i,j,r} = x^t_{i,j} \qquad \forall i,j \in V', t \in T \tag{C.6}$$

$$\sum_{t\in T} x^t_{i,j} + x^t_{j,i} + x^t_{u,v} + x^t_{v,u} \leq 1 \qquad \forall (i,j),(u,v) \in \mathcal{X} \tag{C.7}$$

$$Q - p_j \geq \sum_{r\in R} (q_{i,r} - q_{j,r} + \sum_{t\in T} Q \cdot x^t_{i,j,r}) \qquad \forall i \in V', j \in \bar{V}' \tag{C.8}$$

$$\sum_{i\in V'} \sum_{t\in T} x^t_{i,j,r} = y_{i,r} \qquad \forall j \in V', r \in R \tag{C.9}$$

$$\sum_{j\in V'} \sum_{t\in T} h^t \cdot x^t_{i,j,r} \geq q_{o,r} - q_{i,r} - M \cdot (1 - y_{i,r}) \qquad \forall i \in \bar{V}', r \in R \tag{C.10}$$

$$\sum_{i\in V'} q_{i,r} = q_{o,r} \qquad \forall r \in R \tag{C.11}$$

$$2 \cdot y_{i,r} \leq q_{i,r} \leq Q \cdot y_{i,r} \qquad \forall i \in \bar{V}', r \in R \tag{C.12}$$

$$L - d_{i,j} \geq \sum_{r \in R}(g_{i,r} - g_{j,r} + \sum_{t \in T} L \cdot x^t_{i,j,r}) \qquad \forall i \in V', j \in \bar{V}' \quad \text{(C.13)}$$

$$\sum_{i \in V'} \sum_{t \in T} x^t_{i,j,r} \cdot \tilde{l}^z \geq g_{o,r} - g_{i,r} - M \cdot (1 - y_{i,r}) \qquad \forall j \in V', r \in R \quad \text{(C.14)}$$

$$\sum_{i,j \in V} d_{i,j} x^t_{i,j,r} \leq l_t \qquad \forall t \in T, r \in R \quad \text{(C.15)}$$

$$\sum_{i \in V'} g_{i,r} = g_{o,r} \qquad \forall r \in R \quad \text{(C.16)}$$

$$s_i \cdot y_{i,r} \leq g_{i,r} \leq L \cdot y_{i,r} \qquad \forall i \in \bar{V}', r \in R \quad \text{(C.17)}$$

$$g_{i,r}, g_{o,r} \in \mathbb{Q}^+ \quad \text{(C.18)}$$

$$q_{i,r}, q_{o,r}, p_j \in \mathbb{Z}^+ \quad \text{(C.19)}$$

$$y_{i,r} \in \{0, 1\} \quad \text{(C.20)}$$

$$x^t_{i,j} \in \{0, 1\} \quad \text{(C.21)}$$

$$x^t_{i,j,r} \in \{0, 1\} \quad \text{(C.22)}$$

$$\underline{m} \leq m \leq \overline{m}, \in \mathbb{Z}^+. \quad \text{(C.23)}$$